Supplementary Information (SI) for Physical Chemistry Chemical Physics.

Electronic Supporting Information

Two-Step Insertion/Release of Electrolytic Cations in Redox-Active Hydrogen-Bonding Nanoporous Coordination Crystals

Makoto Tadokoro*, Ryota Nishimura , Hajime Kamebuchi, Fumiya Kobayashi, Jun Miyazaki, and Masa-aki Haga

Contents

METHODS

1. Materials

Crystal **1** was prepared as described in the literature. [1]

2. Solid-state CV measurements

Solid-state CV measurements were performed using a single crystal of **1**, using 0.1 M solutions of each electrolyte in MeCN solution (10 cm^3), with a ϕ~ 3 mm Pt electrode for a working electrode, a Pt wire for a counter electrode, and an Ag/Ag^+ electrode for a reference electrode. Single crystals of about 0.5 mm were fixed on a membrane filter with ϕ~ 3 µm pores. Ar atmosphere was maintained throughout the measurements. The peak area of solid-state CV measurements is calculated with using BAS (ALS/CHI6121B) equipment.

[1] M. Tadokoro, H. Hosoda, T. Inoue, A. Murayama, K. Noguchi, A. Iioka, R. Nishimura, M. Itoh, T. Sugaya, H. Kamebuchi and M. Haga, *Inorg. Chem.,* 2017, **56**, 8513–8526.

3. Molecular structures

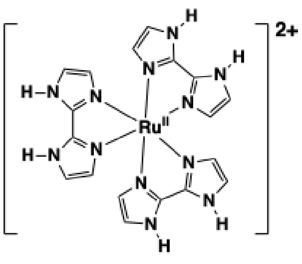

$[Ru^{II}(H_2bim)_3]^{2+}$

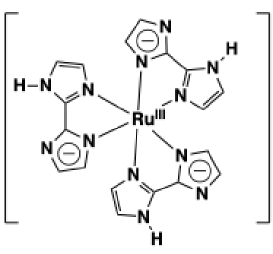

$[Ru^{III}(Hbim)_3]$

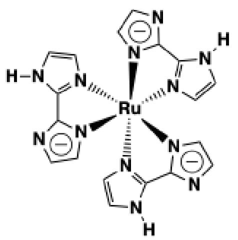

Δ-$[Ru^{III}(Hbim)_3]$

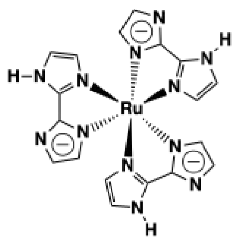

Λ-$[Ru^{III}(Hbim)_3]$

Table S1. Optimized structure, the surface of PCM solvation cavity in acetonitrile condition, and the average distance (angstrom) between H atom of olefin in normal alkyl amine or of benzene in tetraphenyl phosphine and center atom (P or N) in gas phase and acetonitrile.[2]

Molecule	PPh_4	$(n\text{-}C_3H_7)_4N$	$(n\text{-}C_4H_9)_4N$	$(n\text{-}C_5H_{11})_4N$	$(n\text{-}C_6H_{13})_4N$	$(n\text{-}C_7H_{15})_4N$	$(n\text{-}C_8H_{17})_4N$
gas phase	5.69052	4.75690	6.05520	7.32219	8.61490	9.88608	11.17547
Optimized structure	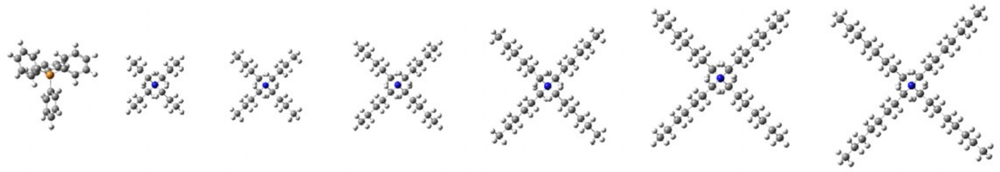						
PCM solvation cavity	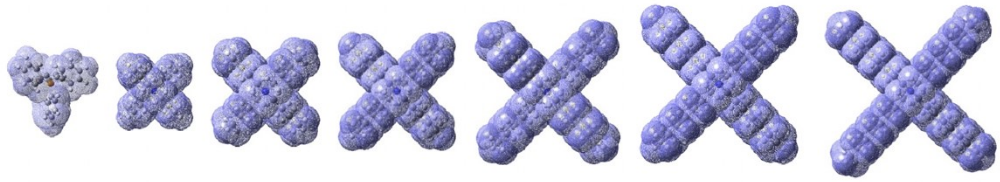						
Solvent	5.69089	4.75034	6.04902	7.31638	8.60913	9.88151	11.17186

We performed the geometry optimization for those molecules in gas phase and PCM condition (solvent: Acetonitrile) using B3LYP/6-311+G(d) basis set included in Gaussian 16 software package[1)]. The temperature was set at 298.15 K every calculation. The illustrations were depicted by Gauss View 6.1.1.

[2] Gaussian 16, Revision C.01, M. J. Frisch, G. W. Trucks, H. B. Schlegel, G. E. Scuseria, M. A. Robb, J. R. Cheeseman, G. Scalmani, V. Barone, G. A. Petersson, H. Nakatsuji, X. Li, M. Caricato, A. V. Marenich, J. Bloino, B. G. Janesko, R. Gomperts, B. Mennucci, H. P. Hratchian, J. V. Ortiz, A. F. Izmaylov, J. L. Sonnenberg, D. Williams-Young, F. Ding, F. Lipparini, F. Egidi, J. Goings, B. Peng, A. Petrone, T. Henderson, D. Ranasinghe, V. G. Zakrzewski, J. Gao, N. Rega, G. Zheng, W. Liang, M. Hada, M. Ehara, K. Toyota, R. Fukuda, J. Hasegawa, M. Ishida, T. Nakajima, Y. Honda, O. Kitao, H. Nakai, T. Vreven, K. Throssell, J. A. Montgomery, Jr., J. E. Peralta, F. Ogliaro, M. J. Bearpark, J. J. Heyd, E. N. Brothers, K. N. Kudin, V. N. Staroverov, T. A. Keith, R. Kobayashi, J. Normand, K. Raghavachari, A. P. Rendell, J. C. Burant, S. S. Iyengar, J. Tomasi, M. Cossi, J. M. Millam, M. Klene, C. Adamo, R. Cammi, J. W. Ochterski, R. L. Martin, K. Morokuma, O. Farkas, J. B. Foresman, and D. J. Fox, Gaussian, Inc., Wallingford CT, 2019.

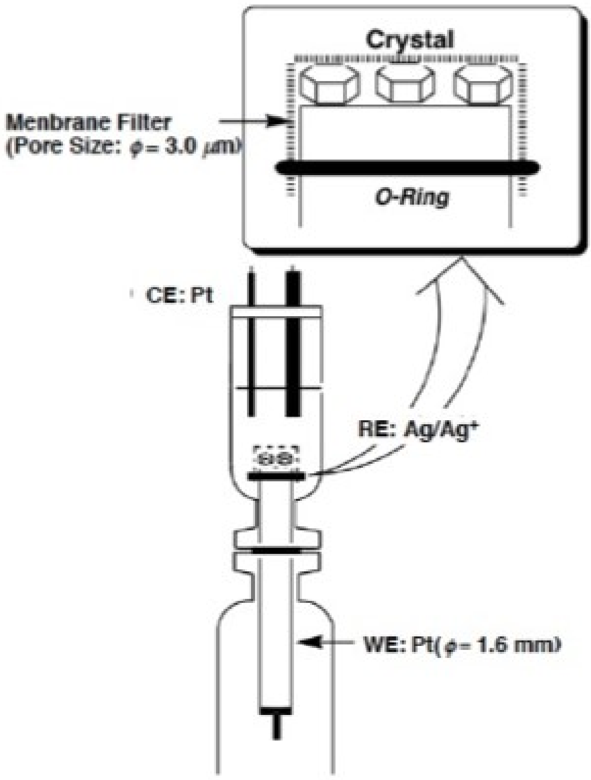

Fig. S1

Schematic representation shows the sold-state CV's cell system, in which some single crystals were fixed on the upward-facing Pt working electrode (ϕ = 1.6 mm) by the membrane filter (a pore size of 3.0 μm). (in MeCN, the concentration of 10^{-3} M)

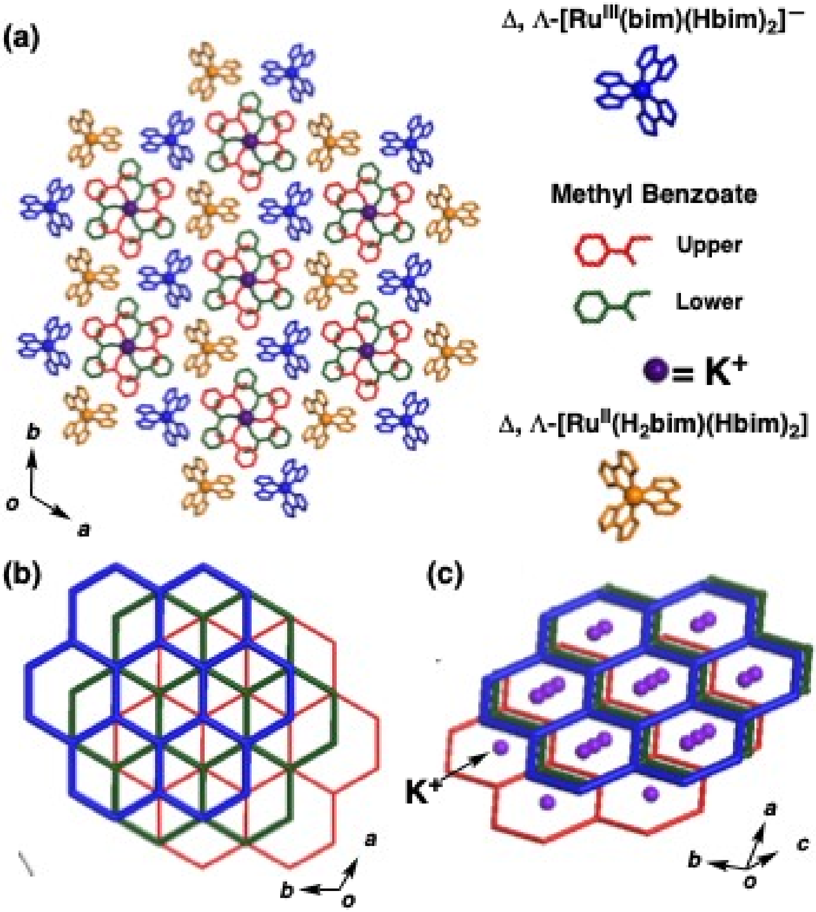

Fig. S2

Crystal structures of **2**. (a) The structure of a honeycomb sheet along the *ab* plane. The blue complexes indicate Δ– or Λ–$[Ru^{III}(bim)(Hbim)_2]^-$, and the yellow complexes also indicate Δ– or Λ– $[Ru^{II}(H_2bim)(Hbim)_2]$. plaplane. The blue complexes indicate Δ–$[Ru^{II}(H_2bim)(Hbim)_2]$. MeOBz coordinated to a K^+ ion (violet sphere) are separated into three upper (red lines) and three lower (green lines) molecules. (b) The crystal structure shows three stacked honeycomb sheets along the *c* axis. (The nearest sheet is shown in thick blue lines, the middle in green lines, and the farthest sheet in thin red lines.) (c) The structure of one of three K^+ ionic arrays at an oblique 45° direction from the *c* axis.

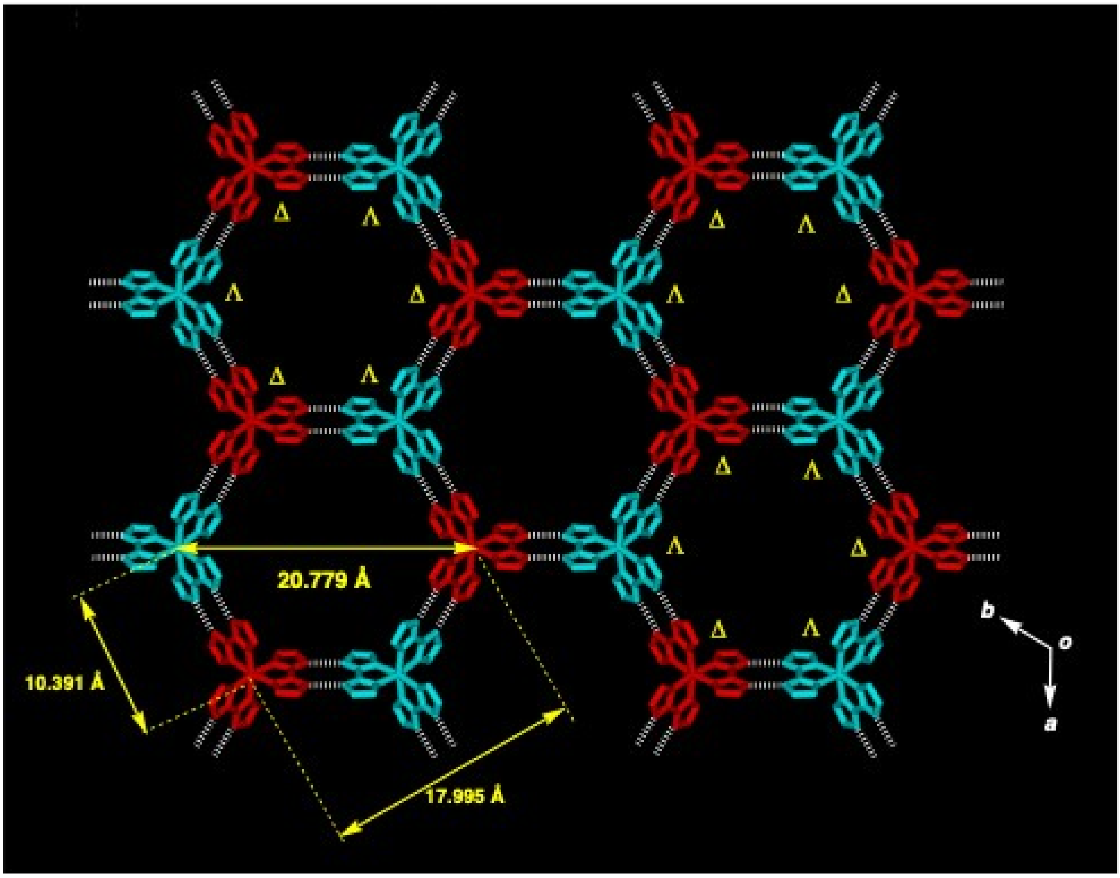

Fig. S3

The crystal structure of a honeycomb sheet in 1 formed by alternating H-bonding between the Δ and Λ optical isomers. The various $Ru^{III}\cdots Ru^{III}$ distances are shown.

(a)

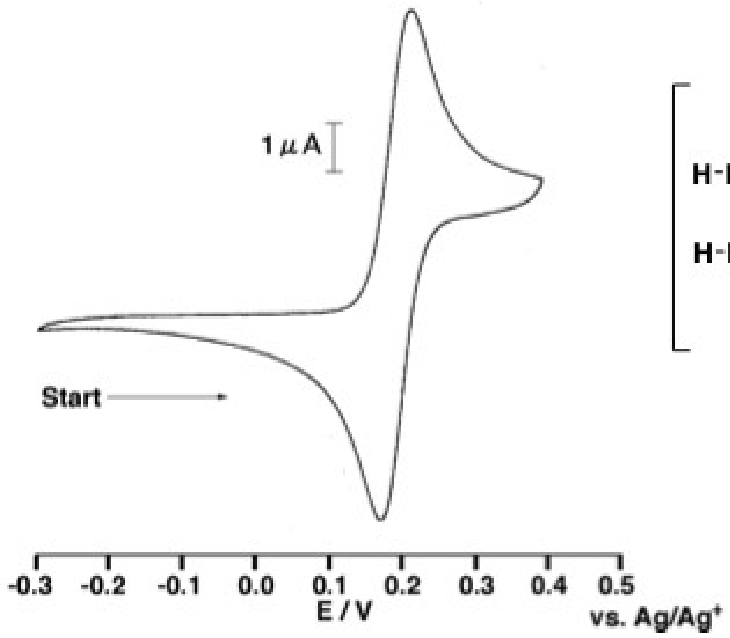

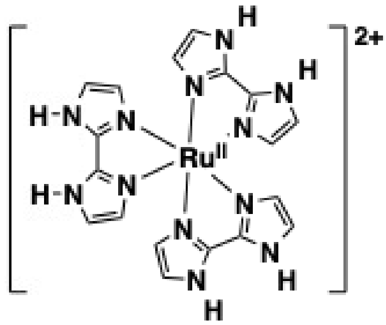

$[Ru^{II}(H_2bim)_3]^{2+}$

Fig. S4

CVs for (a) $[Ru(H_2bim)_3](PF_6)_2$: the completely protonated complex. The redox potentials are $E_{1/2}$ = +0.22 V (vs. Ag/Ag^+).

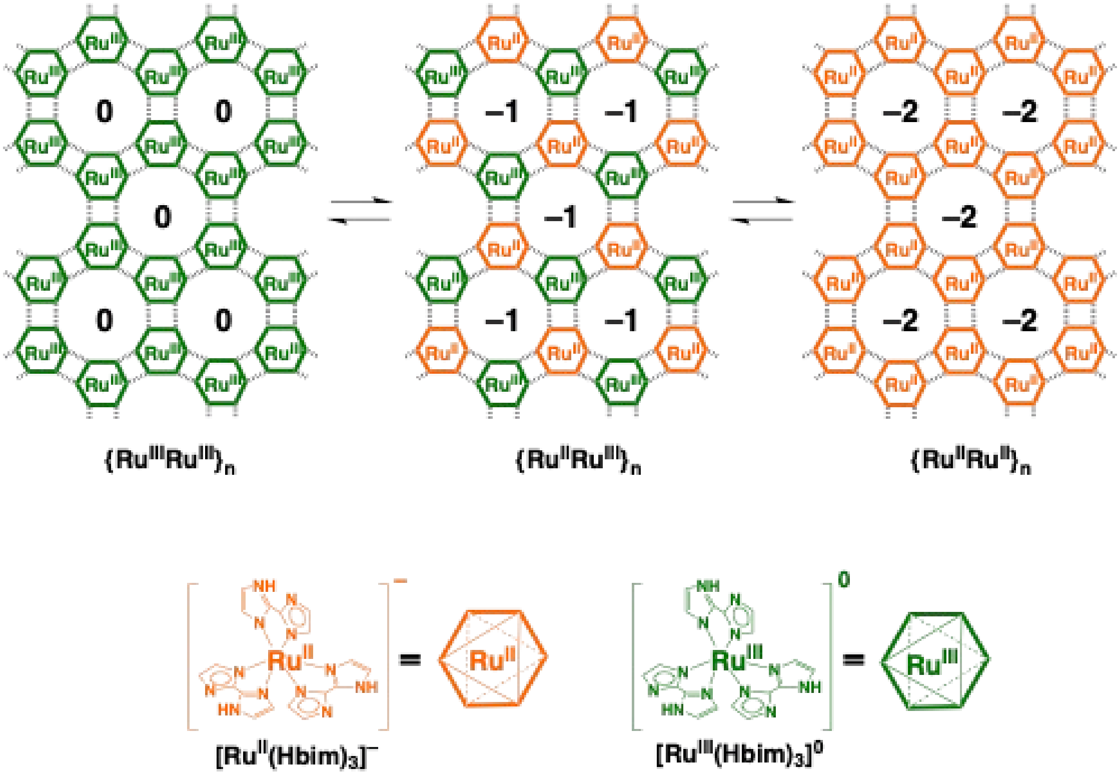

Fig. S5

Electron transfer in **1**. A representative mechanism for the two-step and multi-electron transf observed in the solid-state CV of **1**. $\{Ru^{II}Ru^{III}\}_n$ appears as the alternating reduction of Ru complexes on a honeycomb sheet. The values of 0, –1, and –2 represent the formal char values in the cavity units, respectively.

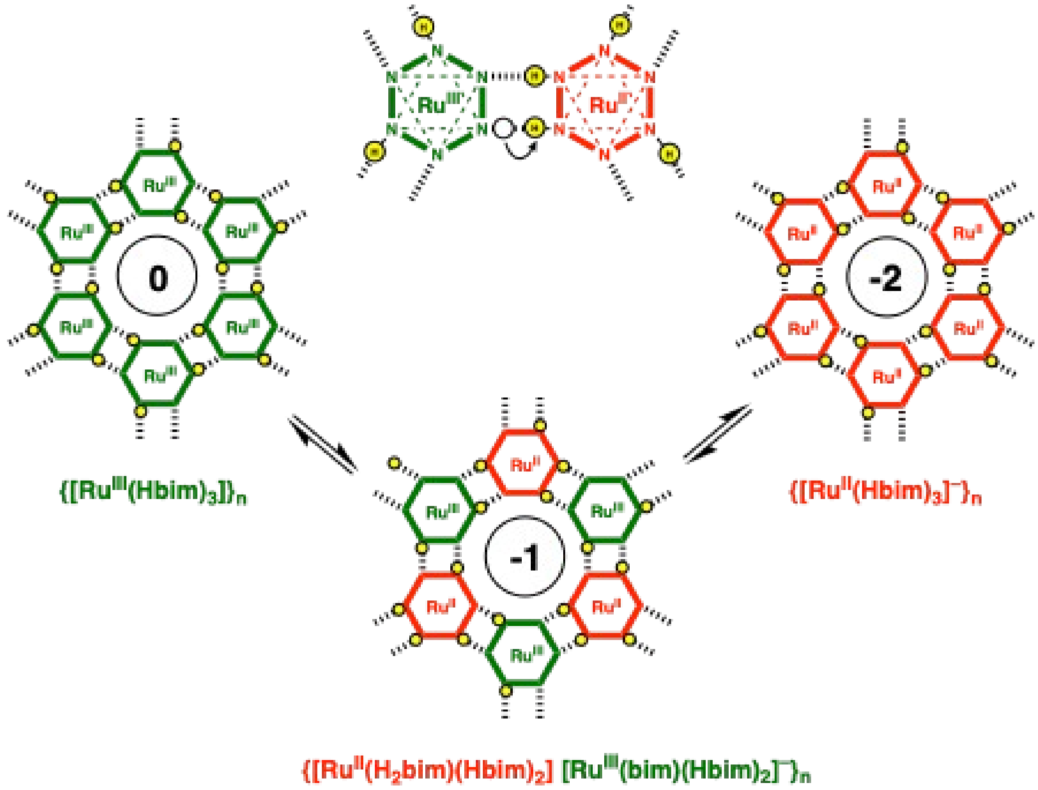

Fig. S6

{Ru^{II}Ru^{III}}$_n$ is alternatingly reduced from **1** to Ru^{II} complexes owing to more rapid proton transfer than the electron transfer from the electrode. As soon as the half of the Ru^{III} complexes of **1** in the honeycomb sheet are firstly reduced to Ru^{II} complexes, a proton transfer from the Ru^{III} complex to a reduced Ru^{II} complex occurs to give {[Ru^{II}(H$_2$bim)(Hbim)$_2$] [Ru^{III}(bim)(Hbim)$_2$]$^-$}$_n$ ({Ru^{II}Ru^{III}}$_n$). In the second reduction step, [Ru^{III}(bim)(Hbim)$_2$]$^-$ reduced a proton is reduced to the Ru^{II} complex, and the Ru^{III}/Ru^{II} reduction potential is shifted to ~0.30 V toward the reductive direction

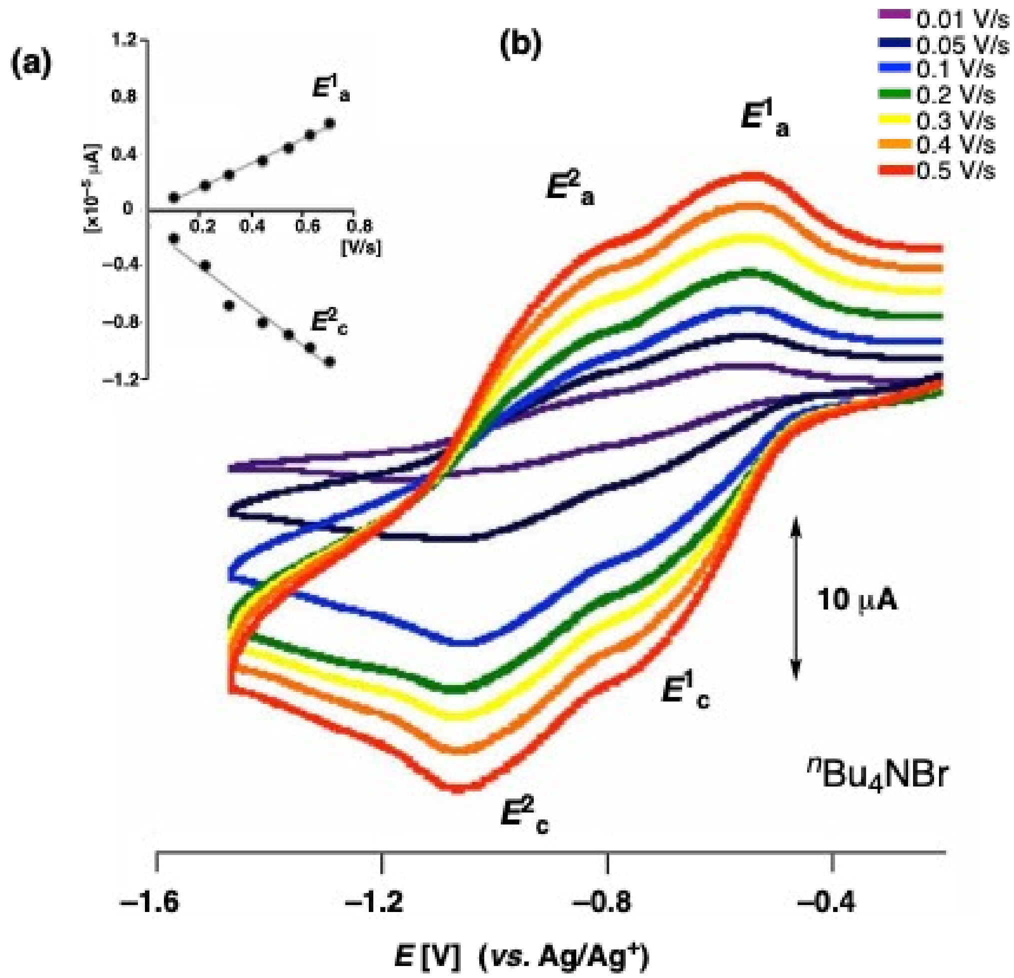

Fig. S7

The solid-state CV image of **1** containing a ^{n}**Bu$_4$NBr** electrolyte salt. (a) The figure shows the plots of current values vs. square root of verocities on $E^1{}_a$ nad $E^2{}_c$, respectively. Since two polts ride in a straigt line, the CV images show a reversible electron transfer. (b) Each CV cycle is measured on the different verocities from 0.01 V/s to 0.5 V/s.

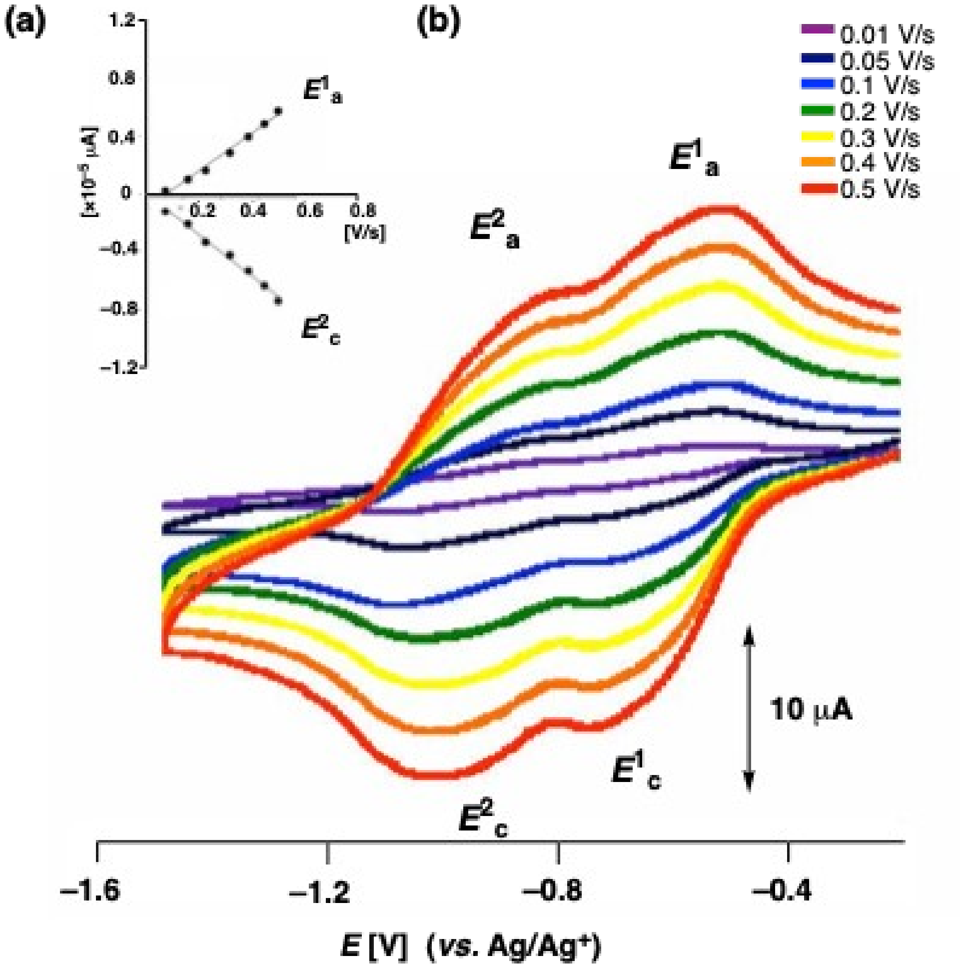

Fig. S8

The solid-state CV image of **1** containing a $^{n}Bu_4NPF_6$ electrolyte salt. (a) The figure shows the plots of current values vs. square root of verocities on E^1_a and E^2_c, respectively. Since two polts ride in a straigt line, the CV images show a reversible electron transfer. (b) Each CV cycle is measured on the different verocities from 0.01 V/s to 0.5 V/s.

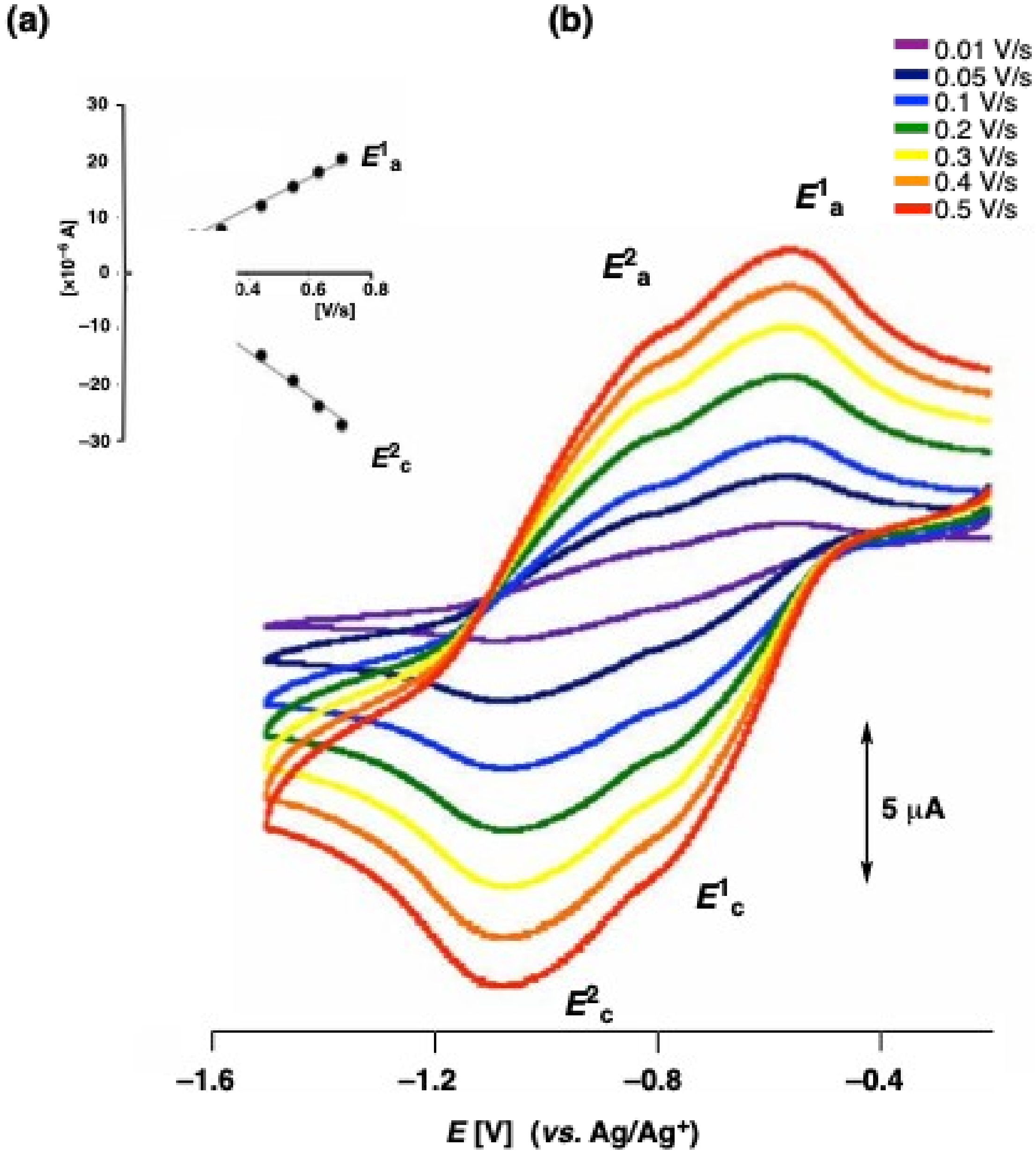

Fig. S9

The solid-state CV image of **1** containing a $^{n}Bu_4NClO_4$ electrolyte salt. (a) The figure shows the plots of current values vs. square root of verocities on $E^1{}_a$ and $E^2{}_c$, respectively. Since two polts ride in a straigt line, the CV images show a reversible electron transfer. (b) Each CV cycle is measured on the different verocities from 0.01 V/s to 0.5 V/s.

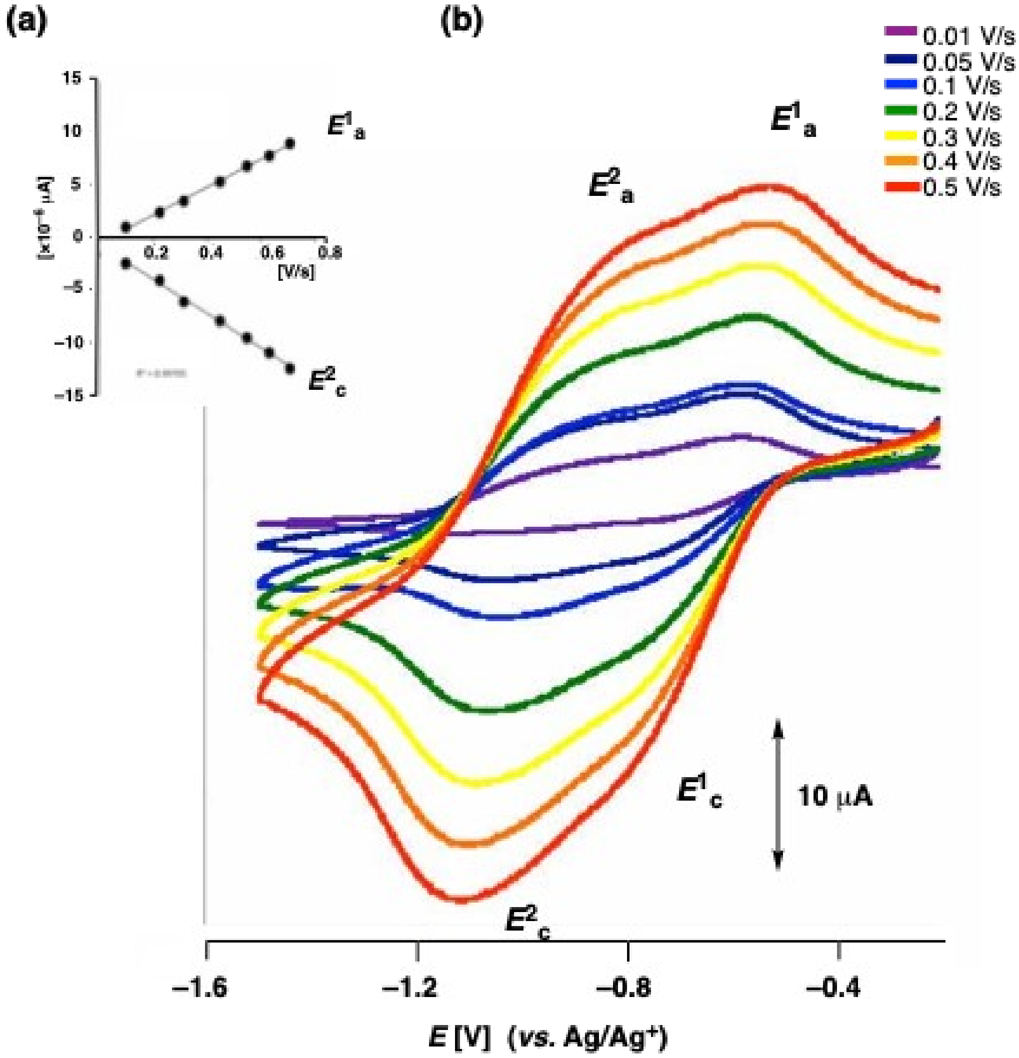

Fig. S10

The solid-state CV image of **1** containing a $^{n}Bu_4NBF_4$ electrolyte salt. (a) The figure shows the plots of current values vs. square root of verocities on $E^1{}_a$ and $E^2{}_c$, respectively. Since two polts ride in a straigt line, the CV images show a reversible electron transfer. (b) Each CV cycle is measured on the different verocities from 0.01 V/s to 0.5 V/s.

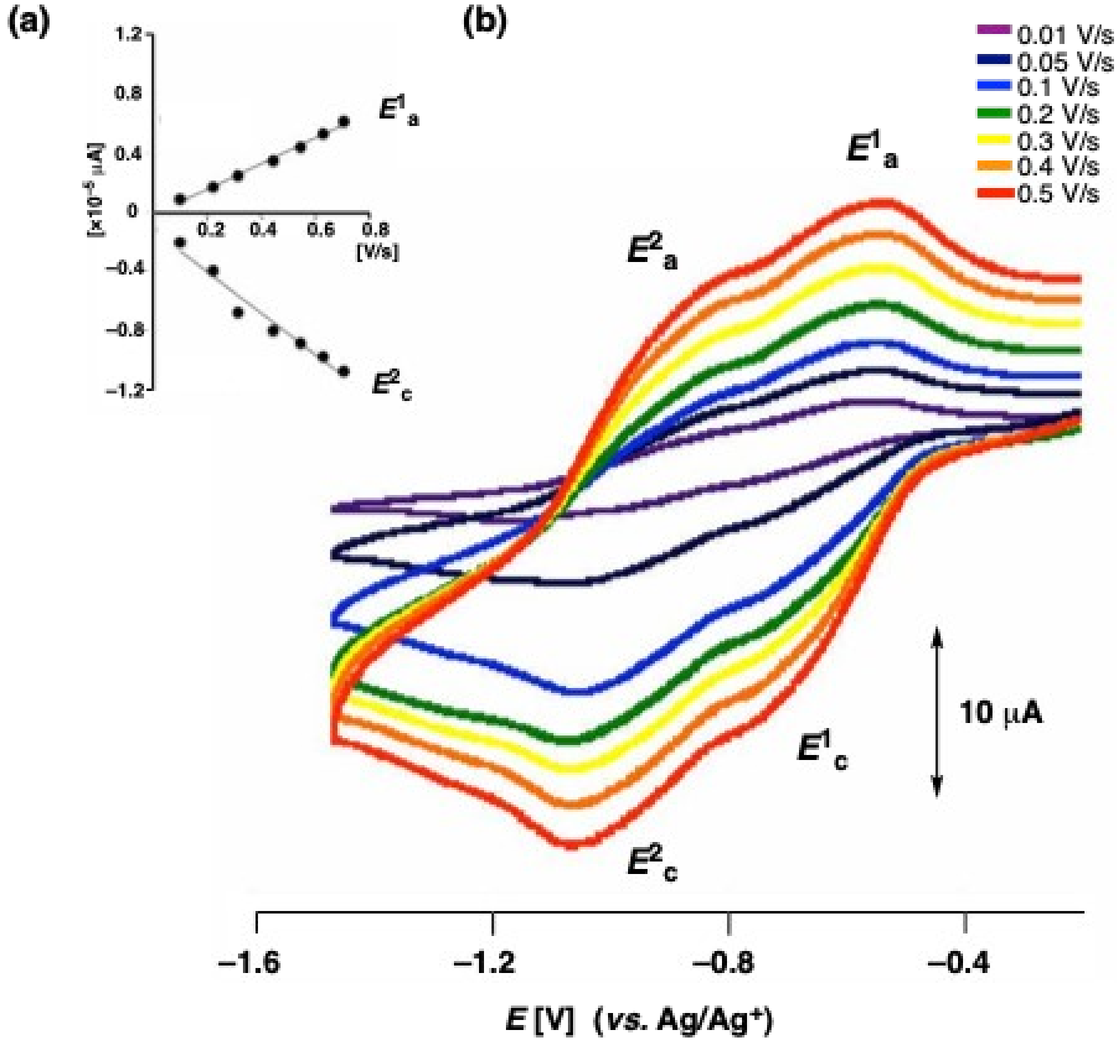

Fig. S11

The solid-state CV image of **1** containing a $^{n}Pr_4NBr$ electrolyte salt. (a) The figure shows the plots of current values vs. square root of verocities on $E^1{}_a$ and $E^2{}_c$, respectively. Since two polts ride in a straigt line, the CV images show a reversible electron transfer. (b) Each CV cycle is measured on the different verocities from 0.01 V/s to 0.5 V/s.

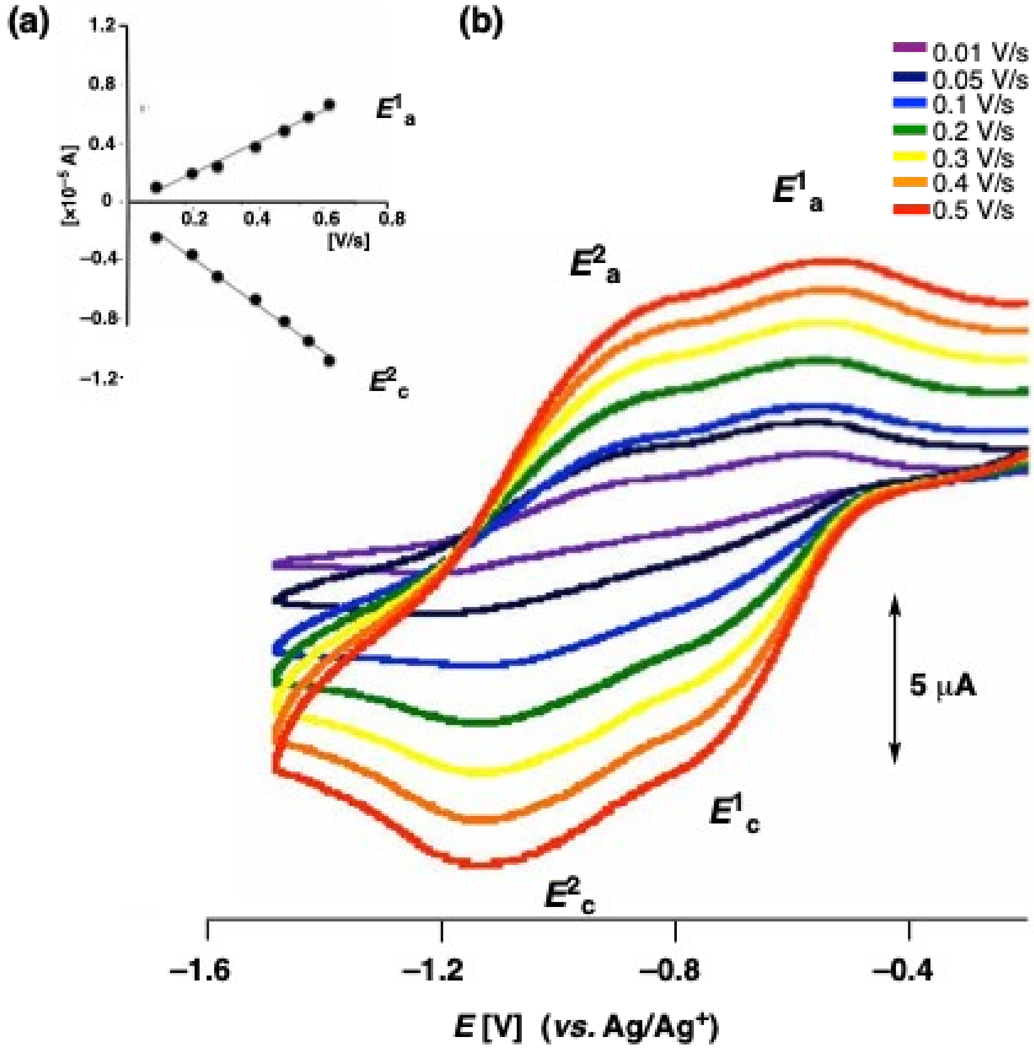

Fig. S12

The solid-state CV image of **1** containing a $^{n}Pen_4NBr$ electrolyte salt. (a) The figure shows the plots of current values vs. square root of verocities on $E^1{}_a$ and $E^2{}_c$, respectively. Since two polts ride in a straigt line, the CV images show a reversible electron transfer. (b) Each CV cycle is measured on the different verocities from 0.01 V/s to 0.5 V/s.

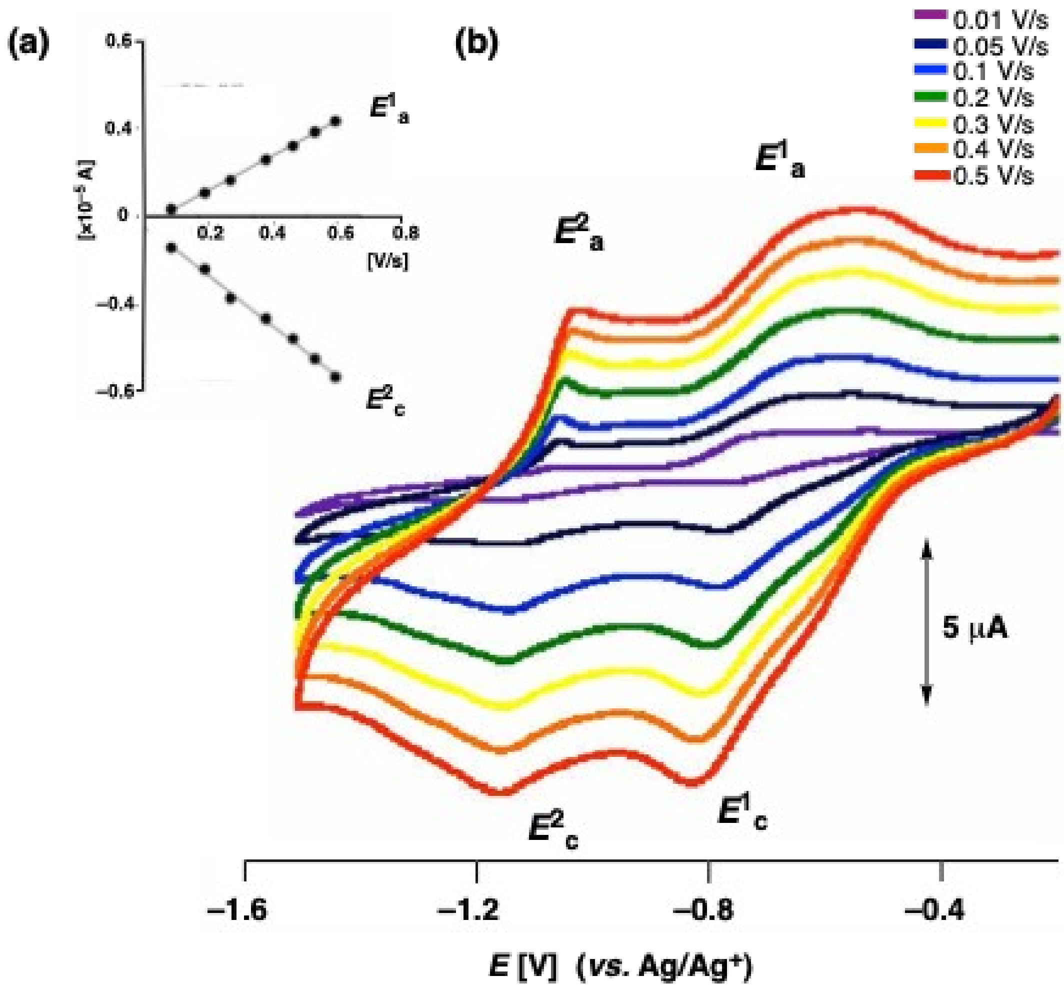

Fig. S13

The solid-state CV image of **1** containing a $^{n}Hex_4NBr$ electrolyte salt. (a) The figure shows the plots of current values vs. square root of verocities on $E^1{}_a$ and $E^2{}_c$, respectively. Since two polts ride in a straigt line, the CV images show a reversible electron transfer. (b) Each CV cycle is measured on the different verocities from 0.01 V/s to 0.5 V/s.

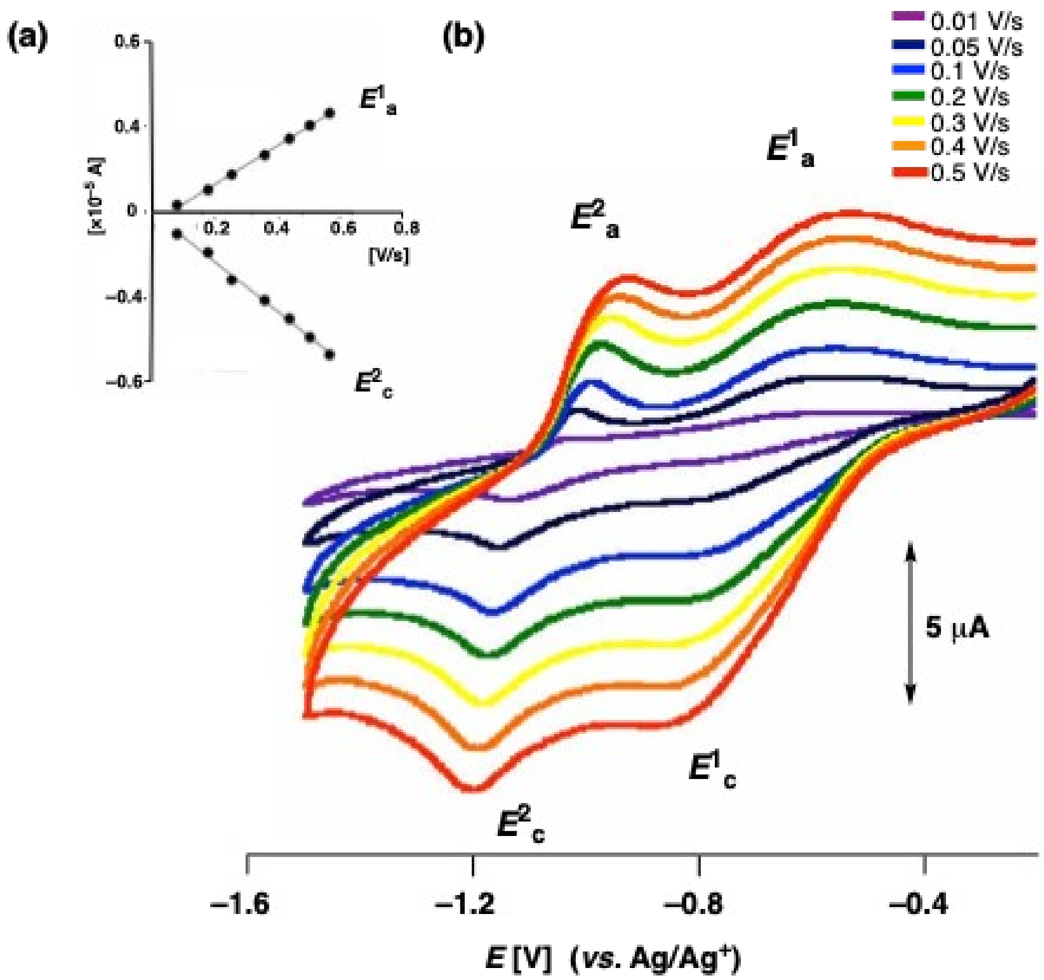

Fig. S14

The solid-state CV image of **1** containing a ^{n}Hep$_4$NBr electrolyte salt. (a) The figure shows the plots of current values vs. square root of verocities on $E^1{}_a$ and $E^2{}_c$, respectively. Since two polts ride in a straigt line, the CV images show a reversible electron transfer. (b) Each CV cycle is measured on the different verocities from 0.01 V/s to 0.5 V/s.

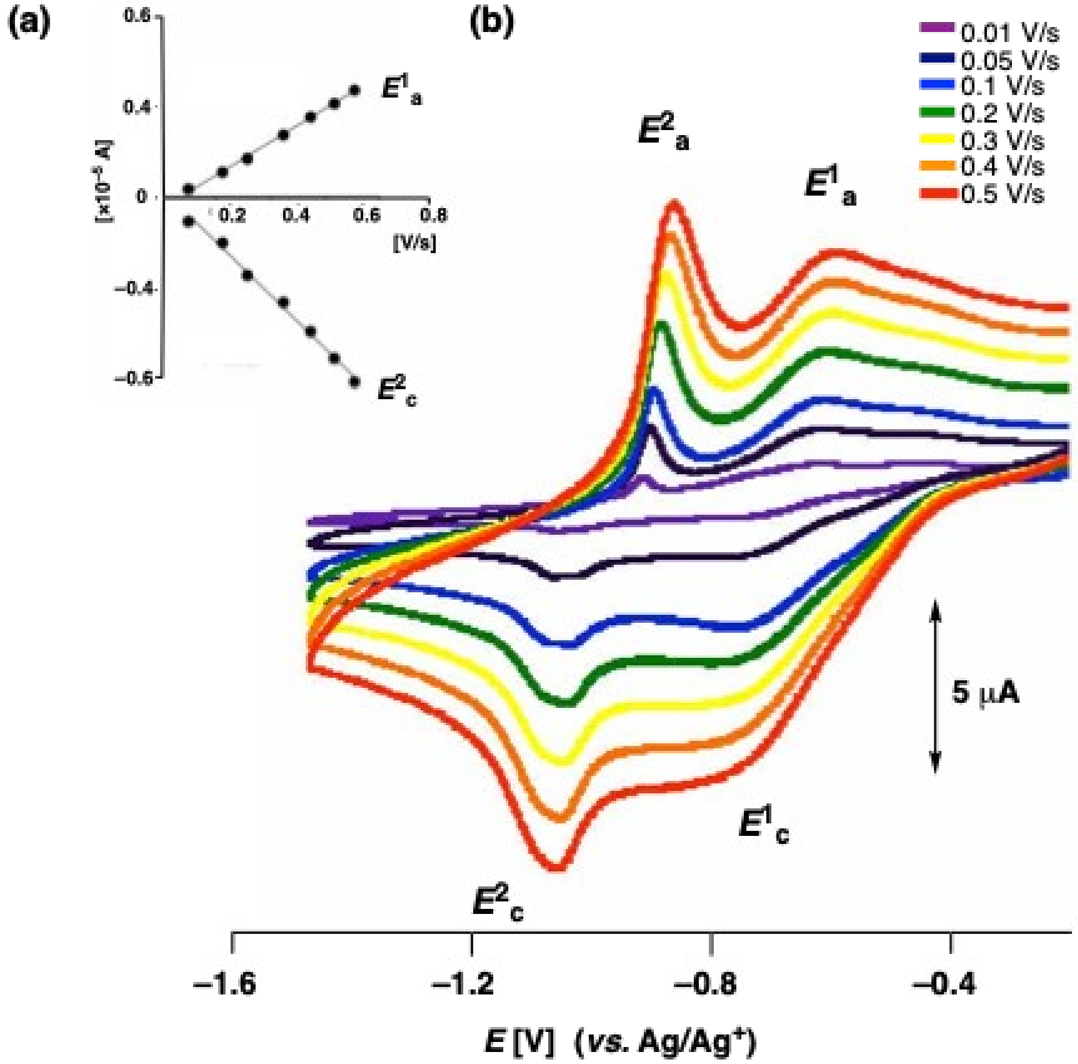

Fig. S15

The solid-state CV image of **1** containing a $^{n}Oct_4NBr$ electrolyte salt. (a) The figure shows the plots of current values vs. square root of verocities on $E^1{}_a$ and $E^2{}_c$, respectively. Since two polts ride in a straigt line, the CV images show a reversible electron transfer. (b) Each CV cycle is measured on the different verocities from 0.01 V/s to 0.5 V/s.

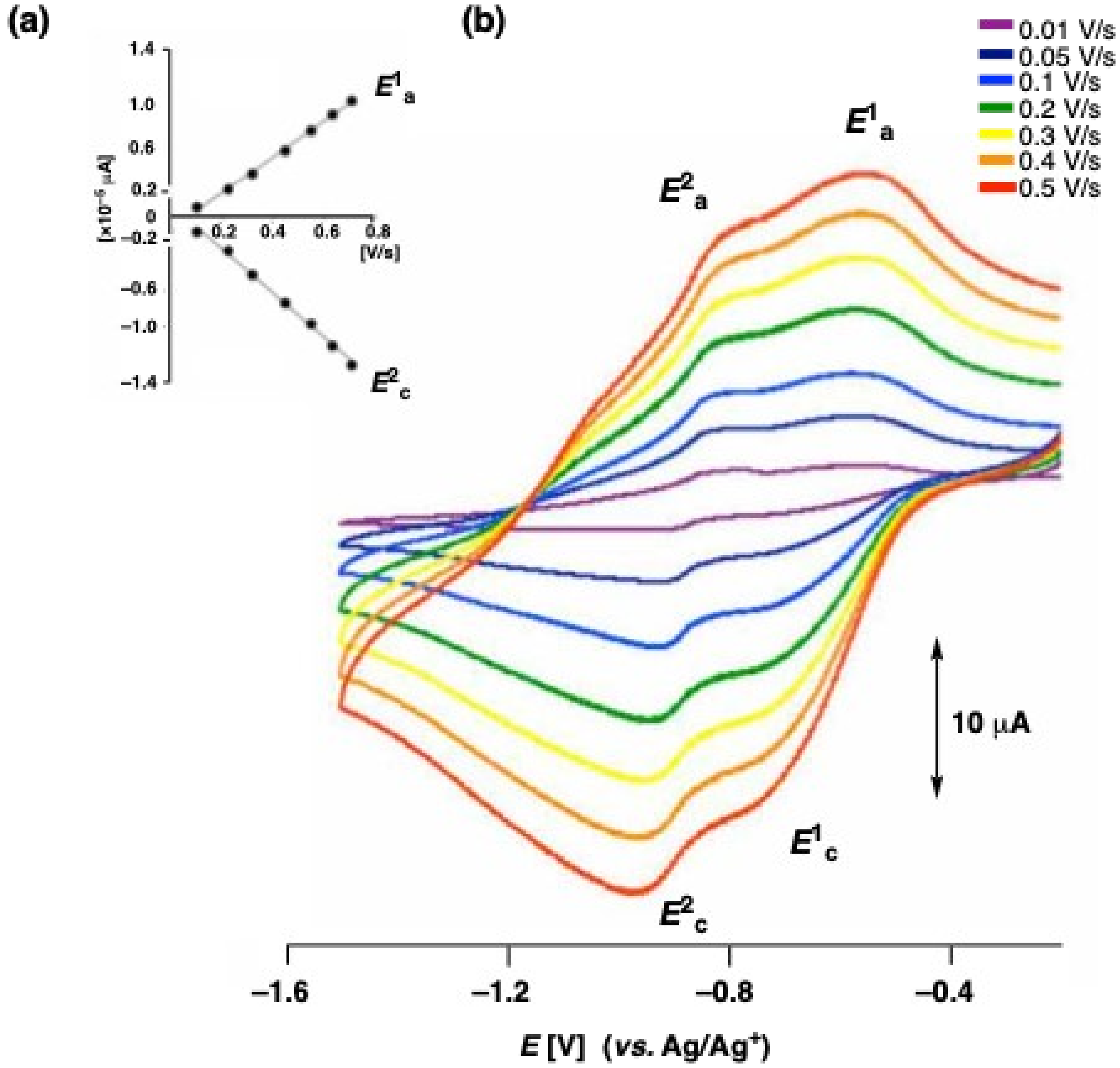

Fig. S16

The solid-state CV image of **1** containing a Ph_4PBr electrolyte salt. (a) The figure shows the plots of current values vs. square root of verocities on $E^1{}_a$ and $E^2{}_c$, respectively. Since two polts ride in a straigt line, the CV images show a reversible electron transfer. (b) Each CV cycle is measured on the different verocities from 0.01 V/s to 0.5 V/s.

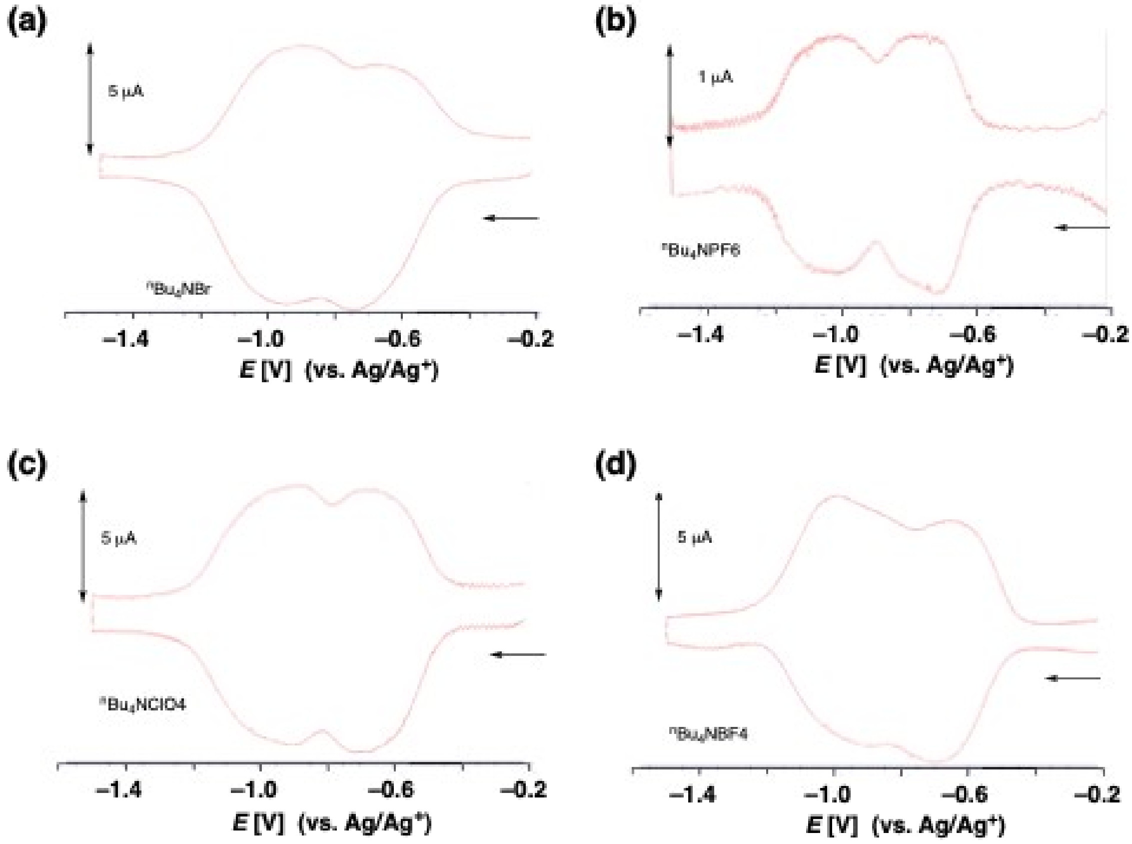

Fig. S17

The semi-differential images of the solid-state CV of **1** on verocity at 100 mV/s (in MeCN, the electrolyte salt 0.1 M) containing (a) $^{n}Bu_4NBr$ (b) $^{n}Bu_4NPF_6$ (c) $^{n}Bu_4NClO_4$ (d) $^{n}Bu_4NBF_4$, respectively.

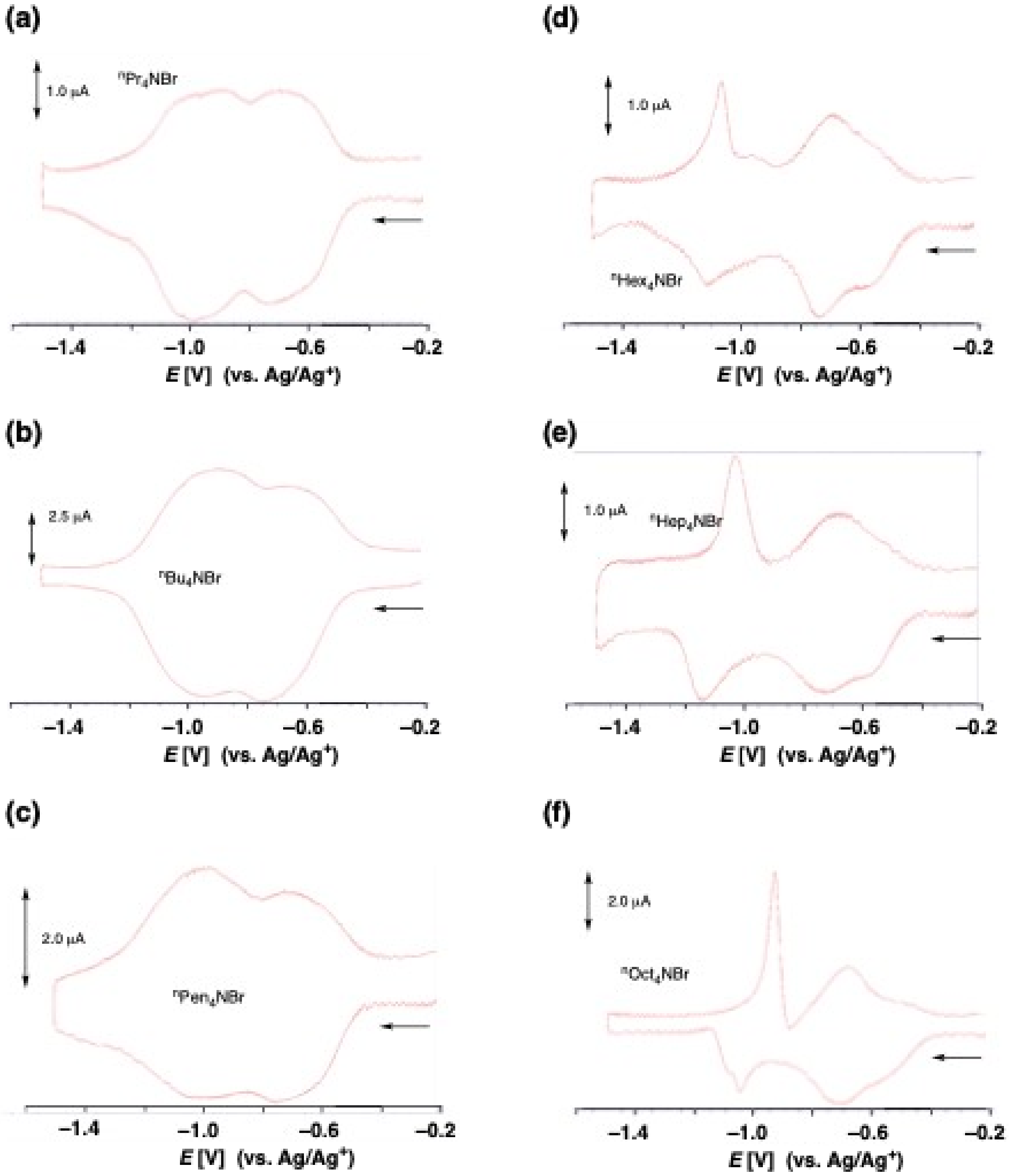

Fig. S18

The semi-differential images of the solid-state CV of **1** on verocity at 100 mV/s (in MeCN, the electrolyte salt 0.1 M) containing (a) $^{n}Pr_4NBr$ (b) $^{n}Bu_4NBr$ (c) $^{n}Pen_4NBr_4$ (d) $^{n}Hex_4NBr$,(e) $^{n}Hep_4NBr$, (f) $^{n}Oct_4NBr$, respectively.